

NUMERICAL INVESTIGATION OF THE INFLUENCE OF FREE STREAM
TURBULENCE ON THE FLOW AROUND A CYLINDER WITH A
DISC LOCATED AHEAD

V. K. Bobyshev and S. A. Isaev

UDC 532.517.4

An analysis is given of the influence of free-stream turbulence of an incompressible fluid on the mechanism of profile drag reduction of bodies with a forward stall zone on the basis of a finite-difference solution of the Reynolds equations.

1. Numerical modelling of the turbulent flow around bodies with discs located ahead of them that are classified as bodies with a forward stall zone (FSZ) has the aim of not only perfecting the mathematical and discrete models to solve complex problems of aero-hydrodynamics but also of obtaining detailed information about the separation flow around such bodies that is, as a rule, inaccessible to physical experiment. The results of numerical computations whose reliability is assured by agreement with available experimental data permit deepening the representation of physical singularities of separation flows of the kind under consideration. In particular, within the framework of a numerical approach to the investigation of the flow around bodies with FSZ it appears possible to determine the influence of such a parameter as the degree of free stream turbulence which is difficult to change in physical experiments, on the flow characteristics.

As has been noted in a number of papers (see [1], say) a significant diminution in the profile drage of bodies as compared with the case of their isolated flow is realized for the axisymmetric turbulent flow around groups of bodies comprised of two discs or a disc and a cylinder. Interaction of the wake behind the disc with the disc or cylinder of greater diameter located downstream can be stable in nature, as tests of models of such bodies performed in aero-hydrodynamic wind tunnels showed [2-4]. The structure of their flow is here determined greatly by the presence of such elements of different scale as viscous shear layers and circulation zones. The sharp edges of the discs and cylinder that turbulize the flow even for comparatively small (on the order of 10^3 - 10^4) Reynolds numbers, result in the built-up of a regime of developed turbulent flow around bodies for which, in particular, a sufficiently weak dependence of the body profile drag on the Reynolds number is characteristic. The complexity of the flow occurring near the mentioned bodies, the interrelation of the components of its structural elements specify the return to numerical modelling of the flow around bodies on the basis of a finite-difference solution of the stationary Reynolds equations that are closed by using the high-Reynolds version of the dissipative two-parameter model of turbulence.

2. Methodological computations performed for separation flows showed the expediency of using the modified dissipative model of turbulence that takes account of the influence of streamline curvature on the turbulence characteristics. As in [4, 5], a correction function f_c of the turbulent Richardson number Ri_T : $f_c = 1/(1 + C_c Ri_T)$ is introduced into the formula for the coefficient of turbulent viscosity ν_T . An additional semi-empirical constant C_c is determined during the methodological experiments from the condition of the best agreement between the computed results and available experimental data and is selected equal to 0.1.

It should be noted that the greatest influence on the quality of the numerical modelling of the flow around the bodies under consideration, for which the formation of a highly intensive circulation zone between the disc and the body behind it is characteristic, is exerted by the effects of numerical diffusion and the assignment of the boundary conditions on the solid surfaces. Thus, it was detected in [6] that the error in computing the frontal drag of two disc can reach 100% when utilizing first order approximation schemes in combination

Civil Aviation Academy, Leningrad. Translated from *Inzhenerno-Fizicheskii Zhurnal*, Vol. 58, No. 4, pp. 566-572, April, 1990. Original article submitted January 17, 1989.

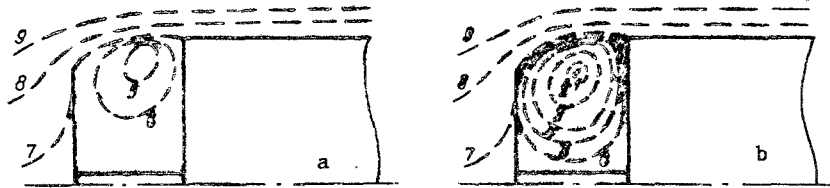


Fig. 1. Patterned of the flow around a body with a forward separation zone obtained when using the method of zero-th diffusion (a) and the method of near-wall functions (b) as boundary conditions on the solid surfaces for 1) $\psi = -0.12$; 2) (-0.11) ; 3) (-0.09) ; 4) (-0.06) ; 5) (-0.03) ; 6) (-0.01) ; 7) 0.005 ; 8) 0.10 ; 9) 0.25 .

with rough practical grids matched with the contour of the body being streamlined. In order to avoid distortions of the numerical solution induced by errors in discretization of the convective terms of the transport equations to a significant degree, it is proposed to utilize a scheme with diminished numerical diffusion in the algorithms to compute turbulent separation flows and, a quadratic Leonard counterflow scheme in particular (see [6], say). In order to assure higher stability of the calculational process here, as in the case of numerical modelling of the laminar flow around bodies with FSZ [3], a modification of this scheme is used that is related to achieving diagonal predominance of the coefficient matrix of the resulting algebraic equations. As in [6], the difference analogs of differential equations for the turbulence characteristics are written on the basis of a hybrid scheme combining central and counterflow unilateral differences. The algorithm for the solution of the problem is constructed within the framework of the splitting concept according to physical processes with reliance on the pressure correction procedure SIMPLE that is extensively used in the practice of engineering computations. The algebraic equations in each iteration step are solved by an explicit-implicit method of linear scanning that combines utilization of a three-point factorization along radial lines with the Gauss-Zaidel' relaxation procedure in the axial direction. Convergence of the iteration process is determined by smallness of the change in the profile drag coefficient of the body, by the tendency of the maximal increments of the stream parameters and the turbulence characteristics to zero.

3. The selection of acceptable, sufficiently correct boundary conditions on the solid surfaces [7] during computation of the turbulent separation flows is not unique, and as a rule, was considered up to now as insulated from the numerical diffusion problem. The necessity of assigning non-trivial boundary conditions follows from the complexity of the technical realization on modern electronic computers with very limited resources of the adhesion condition, as well as from the inapplicability of a high-Reynolds dissipative model of turbulence in direct proximity to the wall. Utilization of the local equilibrium hypothesis in a fully developed turbulent near-wall flow permitted development of a method of near-wall functions that is used extensively in computer practice. However, it should be acknowledged that the acceptability of this method in the separation flow case is validly subjected to doubt since the assumptions on which it is based are not satisfied in the attached flow zone, i.e., near the stagnation points on the body surface. The search for rational methods of formulating the boundary conditions resulted in the idea of a negligibly small diffusion flux from the solid wall that was realized in [5] in particular. It is expedient to estimate the acceptability of the mentioned approaches for modelling the flow around bodies with FSZ.

Computations of the flow around a semi-infinite cylinder with a forward disc were performed for an optimal lay-out ($d = \ell = 0.75$), characterized by minimal profile drag, for several values of the degree of free stream turbulence (from 0 to 1%). The radius of the cylinder, the free-stream velocity and density were selected as parameters to make the variables dimensionless. The turbulence characteristics on the entrance boundary were varied by starting from given magnitudes of the turbulence level and the turbulence scale corresponding to flows obtained in different wind tunnels. The radius of the connecting rod was selected equal to 0.12 and the Reynolds number as $Re = 10^5$. The influence of the disc thickness was not taken into account in the computations. A chessboard type computational grid with grid lines parallel to the coordinate directions contained $50 \cdot 36$ nodes distributed with concentration in the neighborhood of the bodies being streamlined and their sharp edges (size of minimal grid spacing is 0.02). The traditional "soft" boundary conditions for the solution of such problems were given on the exit boundaries of the computational domain (see [4, 6], say).

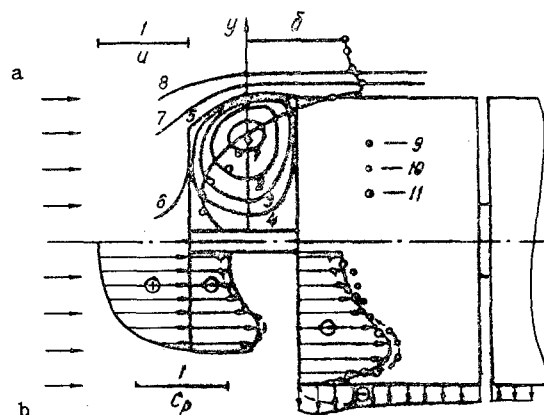


Fig. 2. Streamline pattern of the average flow (a), the profile of the axial velocity component u in the middle section of the cavern between the disc and the cylinder endface (b) and surface distributions of the pressure coefficient C_p on the disc and cylinder (c) for $Tu = 0.5\%$; 1) $\psi = -0.09$; 2) (-0.05) ; 3) (-0.03) ; 4) (-0.01) ; 5) 0.0 ; 6) 0.005 ; 7) 0.10 ; 8) 0.25 ; 9) experimental data for u [2]; 10) experimental data for C_p [2]; 11) experimental data for C_p [4]. The dashed computed curve in Fig. 2c corresponds to $Tu = 0.05\%$.

The flow patterns in a FSZ are compared in Fig. 1 for the selected disc-cylinder layout when using the methods of zero diffusion and near-wall functions, respectively, in the computations. Not taking account of the diffusion flux from the wall in the first case results in a significant diminution of the large-scale vortex intensity, and as a result, to equilibration of the pressure distributions on the endface surfaces of the disc and cylinder in the FSZ. Consequently, the profile drag coefficient of the body turns out to be exaggerated strongly ($C_{xp} = 0.06$), which is in agreement with analogous exaggeration of the frontal drag coefficient for two sequentially arranged discs [6]. Consequently, the method of near-wall functions is utilized in the subsequent computations.

4. Computed results for $Tu = 0.5\%$ are compared in Figs. 2, 3 and the table with experimental data on local stream parameters and turbulence characteristics obtained in a hydraulic tunnel by using a laser-Doppler velocimeter and on the basis of tests of drained models in wind tunnels with a different degree of blocking the tunnel working section by a body α [2, 4]. Experimental data on the total force loads $C_{xp} + C_{xf}$ acting on the measuring element of length $\lambda = 1.25$ connected with strain-gauge balances embedded in the cylindrical part of the model (with the influence of the correction α taken into account are represented in the table [2] as well as those measured by the strain-gauge balances on a model with cylindrical part aspect ratio $\lambda = 9$ (without taking account of the contribution of the base drag). Estimation of the profile drag coefficient C_{xp} is executed in [2] in the first case on the basis of an assumption on the equality of the mean value of the local friction on the lateral surface of the measuring element to the experimentally determined maximal values of the turbulent stresses in the shear layer. Results of computations of the flow around a cylinder with the same geometry of the disc probe are presented in the same table.

The streamline pattern represented in Fig. 2a for the average flow shows formation of a stable large-scale toroidal vortex in the cavern between the disc and cylinder endface. The vortex center located in the cavern middle plane turns out to be shifted towards the separating streamline connecting the sharp edges of the disc and the cylinder so that the flow in the vortex possesses the highest intensity in the shear layer domain on the FSZ boundary as well as in the circumferential domain from the edge of the cylinder endface surface. Indeed, there follows from the distribution of the longitudinal velocity component u in the cavern middle section that (Fig. 2b) the maximal magnitude of the reverse flow velocity near the connecting rod is 50% of the free-stream velocity (it is a quantity of the order of 0.35 for $Re = 10^3$ in the laminar mode [3]). At the same time, the maximal magnitude of the radial

TABLE 1. Comparison Between Experimental and Computed Results for the Frontal Drag and its Components for a Disc-Cylinder Layout $d = \ell = 0.75$

Data	Tu, %	α	λ	C_{xp}	$C_{xp} + C_{xf}$
Experiment	0,5	0,03	1,25	$0,03 \pm 0,005$	$0,04 \pm 0,005$
	0,5	0,006	9	—	0,11
Computation	0,5	0,003	1,25	0,031	0,051
	0,5	0,003	9	0,031	0,094
	0,05	0,003	1,25	0,020	0,038

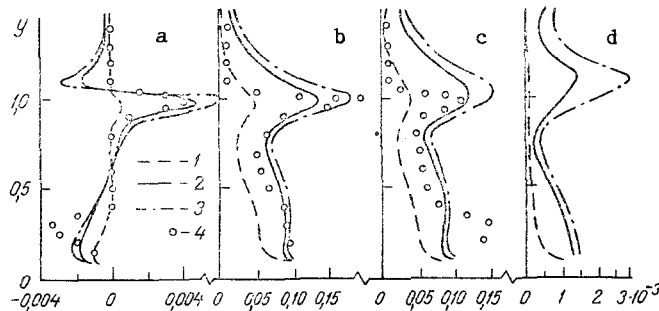


Fig. 3. Distributions in the middle section of the cavern between the disc and cylinder for the turbulent friction stress $-\overline{u'v'}$ (a), the fluctuating axial $\sqrt{u'^2}$ (b) and radial $\sqrt{v'^2}$ (c) velocity components, the coefficient of kinematic turbulent viscosity ν_T (d): 1) $Tu = 0.05\%$; 2) 0.5% ; 3) 1.0% ; 4) experiment [2], $Tu = 0.5\%$.

velocity component v near the circumferential part of the cylinder endface turns out to be near to or to exceed the free-stream velocity.

The high intensity of the flow in a large scale vortex in turn specifies the presence of a strong rarefaction zone on the cavern surface, where the maximal values of the static pressure coefficient C_p are, as follows from Fig. 2c, close to, in absolute value, or exceed the pressure at the stagnation point on the forward disc, i.e., greatly exceed the rarefaction level in the near wake behind a blunt body ($C_{p \min}$ on the back side of a disc around which a uniform stream flows with the degree of turbulence under consideration, is -0.42 while $C_p = -1.03$ on the endface of a cylinder with a disc for $d = \ell = 0.75$). At the same time, the maximal rarefaction is the quantity -0.74 in the laminar mode of the flow around a body of this geometry for $Re = 10^3$. The strong nonuniformity in the local force load distributions on the endface surfaces of the disc and cylinder, related to the flow inhomogeneity in the vortex and the notable equilibration of the pressure in the domain adjoining the connecting rod should be noted; an analogous pattern is observed in the laminar case [3], but in a less definite form.

The strong rarefaction in the vortex, in combination with the smooth nature of the flow around the cylinder side surface caused by flow attachment to its sharp edge, predetermines origination of a pulling force of considerable magnitude from the cylinder endface surface acting in the opposite direction relative to the frontal drag force and almost completely compensating the force load on the disc projecting ahead of the cylinder. Consequently, the profile drag of the layout becomes almost two orders lower than the drag of the composite bodies and approximates the profile drag of a streamlined body ($C_{xp} 0.02$).

Analysis of the turbulence characteristics whose distribution in the middle section of the cavern is shown in Fig. 3, permits a more detailed investigation of the nature of the large-scale vortex, and supplementing the representation of the mechanism of its influence on the local and integral parameters of a flow of the type under consideration. The characteristic elements of the flow configuration due to viscous effects and playing a substantial part in this mechanism are the turbulent shear layers being developed along the separation

domain boundary, on the cavern walls, and on the cylinder side surface. As is seen from the friction stress profile $-\overline{u'v'}$ (Fig. 3a), the maximal values of $-\overline{u'v'}$ are realized in zones of shear layer location while the quantities $-\overline{u'v'}$ are negligibly small at the center of the vortex and in the free stream domain at the same time. Hence, there is a foundation to assume the model proposed by Batchelor, according to which the vortex can separate into two zones, an inviscid core and a comparatively thin surrounding shear layer, to be sufficiently valid for the large-scale vortex flow under consideration. The maximal magnitudes of the fluctuating components of the velocity are also realized in the shear layer at the FSZ boundary (Fig. 3b and c), which results in a local maximum in the same domain of the kinematic viscosity ν_T . It is interesting to note that the mean level of the fluctuating velocity component magnitudes governing the turbulence intensity in a large-scale vortex is approximately 0.05-0.10 of the free-stream velocity, which exceeds analogous quantities in the stream impinging on the body by an order ($Tu = 0.5\%$). Therefore, a large-scale vortex in the FSZ enters the role of turbulence generator, however, the turbulence pumping level in the case of a layout optimal in the profile drag is almost 3 times lower as compared with the flow in the near wake behind a blunt body.

Comparison of the computed and experimental results of the flow around a cylinder with a disc of this geometry shows their good agreement in the stream local and integral parameters and completely satisfactory agreement in turbulence characteristics.

5. As is known, the degree of free-stream turbulence plays a very important role in the transfer of experiment results conducted on models to full-scale conditions corresponding to a real object. The fact is that a comparatively high degree of stream turbulence under laboratory conditions, in particular, in wind tunnels, results in accelerated turbulization of the boundary layer on the surface of smooths treamlined bodies and, therefore, to an increase in the friction drag comprising the main part of the body frontal drag. Therefore, the influence of external turbulence for smooth bodies reduces to growth of their frontal drag because of the increase in viscous friction. The influence becomes most noticeable for Tu on the order of 1-2% and higher.

For bodies of revolution with FSZ the external turbulence results in not only a change in the friction drag but also exerts noticeable influence on their profile drag even for comparatively moderate Tu values. As follows from the results presented in the table, a change in the degree of free-stream turbulence by an order of magnitude, starting with $Tu = 0.05\%$, results in a 1.5 times increase in C_{xp} while C_{xp} grows 3 time for $Tu = 1.0\%$. As Tu grows, a drop occurs in the intensity of the large-scale vortex in the cavern between the disc and the cylinder (the maximal value of the stream function in the vortex is $\psi_m = -0.12$, for $Tu = 0.05\%$ while $\psi_m = -0.10$ for $Tu = 1.0\%$); the point of attachment of the separating streamline is shifted down along the endface from its sharp edge, the return flow velocity in the cavern diminishes as does the rarefaction level in the vortex. The mentioned changes are due to growth of the shear layer being developed on the boundary of the separation domain. As is seen from Fig. 3, an increase in Tu from 0.05 to 0.5% raises the level of turbulent viscosity by more than an order in the middle section of the shear layer. Therefore, growth of the profile drag of a body of disc-cylinder configuration is associated with FSZ deformation due mainly to the flow change in the shear layer.

The substantial influence disclosed for the degree of free stream turbulence on the local and integral flow characteristics in the neighborhood of a body with a FSZ indicates the necessity for correcting the data obtained in wind tunnels with a sufficiently high degree of turbulence of the stream being formed therein ($tu = 0.5-1.0\%$). The computation performed showed that it is desirable to use wind tunnels with a low level of stream turbulence (on the order of 0.05% and below) for the experimental investigation of separation flows of this kind.

NOTATION

x, y is the axial and radial coordinates; d is the disc diameter; l is the gap between the disc and the cylinder; R is the cylinder radius; λ is elongation of the cylindrical part of the model; α is the degree of model blocking the tunnel working section; u, v, Tu are the axial and radial velocity components and the degree of free-stream turbulence; $-\overline{u'v'}$, $\sqrt{u'^2}$, $\sqrt{v'^2}$ are Reynolds stress tensor components; ψ is the stream function of the average flow; k is the turbulent fluctuation energy; ε is the rate of turbulent energy dissipation; ν is the coefficient of kinematic viscosity; Re is the Reynolds number; Ri is the Richardson

number; C_c is a semi-empirical constant; C_x , C_{xp} , C_{cf} are the frontal, profile, and friction drag coefficients. The subscript T is for turbulence.

LITERATURE CITED

1. I. A. Belov, Interaction of Nonuniform Streams with Obstacles [in Russian], Leningrad (1983).
2. K. Koenig and A. Roshko, J. Fluid Mech., 156, 167-204 (1985).
3. V. K. Bobyshev, S. A. Isaev, and O. L. Lemko, Inzh.-Fiz. Zh., 51, No. 2, 224-232 (1986).
4. V. K. Bobyshev and S. A. Isaev, Turbulent Transfer Processes [in Russian], 39-48, Minsk (1988).
5. M. A. Leshtsiner and W. Roddy, Trans. ASME. Theor. Prin. Eng. Comp., 103, No. 2, 299-308 (1981).
6. S. A. Isaev, Inzh.-Fiz. Zh., 48, No. 6, 918-921 (1985).
7. I. A. Belov and N. A. Kudryavtsev, Pis'ma Zh. Tekh. Fiz., 7, NO. 14, 887-890 (1981).

HELICAL WAVES IN A LIQUID FILM ON A ROTATING DISK

G. M. Sisoiev and V. Ya. Shkadov

UDC 532.516

The stability of steady-state axisymmetric flow against non-axisymmetric perturbations is considered.

A number of experimental and theoretical studies have been made on wave generation in a liquid film moving on the surface of a rotating flat disk [1-7]. The stability of the limiting stationary solution for a relatively thin film was studied in [2, 3, 6, 7], using an asymptotic method [2, 3, 7] or a numerical method [6]. In this paper we study the stability of the main flow, for which the Ekman number [2] is finite; we can point out that interest in such modes stems from the desire to increase the productivity of technological processes employing the given form of film flow.

Suppose that a viscous incompressible liquid is fed at a constant flow rate Q near the center of a rotating disk. The flow of the film formed on the disk is described by the functions

$$u = \frac{u_r}{\Omega r \delta^2}, \quad v = \frac{1}{\delta^2} \left(\frac{u_\theta}{\Omega r} - 1 \right), \quad w = \frac{u_z}{\Omega H_c \delta^2}, \quad p = \frac{p_f}{\rho \Omega^2 H_c^2}, \quad h = \frac{h_f}{H_c},$$

where $\delta = H_c \sqrt{\Omega/\nu}$, and δ^{-2} is the Ekman number. As independent variables we use the quantities $x = \ln(r/R)$, θ , $y = z/H_c$ and $s = \Omega t/\delta^2$. The system of equations and boundary conditions for determining u , v , w , p , and h is given in [3].

The hypothesis of local plane-parallelism [3] is used to study the stability of steady-state axisymmetric flow $U_1(x, y)$, $V_1(x, y)$, and $H_1(x)$, obtained numerically [8], in which the initial thickness of the film at $r = R$ is used as the characteristic quantity H_c ; the non-stationary solution in this case is written as [6]

$$u(x, \theta, y, s) = U_1(x_0, y) + H_0^2 u_1(\xi, \theta, \eta, \tau), \quad v = V_1 + H_0^2 v_1, \quad (1)$$

$$w = \frac{H_0^2}{\varepsilon_0} w_1, \quad p = \frac{H_0}{\varepsilon_0} p_1, \quad h = H_1 + H_0 h_1,$$

where $x_0 = \ln(r_0/R)$, $H_0 = H_1(x_0)$, $\varepsilon_0 = \varepsilon(x_0)$, $\xi = (x - x_0)/(\varepsilon_0 H_0)$, $\eta = y/H_0$, and $\tau = s/H_0^2$. Substituting solution (1) into the initial equations and boundary conditions and linearizing, we obtain a problem for small perturbations, which have wave solutions of the form $f_1(\xi, \theta, \eta, \tau) = \hat{f}_2(\eta) \exp i(\alpha \xi + n\theta - \omega \tau)$, where $\tau_1 = \text{Re} \tau$, $\text{Re} = U_* H_* / \nu$, $H_* = H_c H_0$, and $U_* = r_0 \Omega^2 H_*^2 / \nu$. After some manipulations, we can obtain the following problem for amplitude functions:

M. V. Lomonosov State University, Moscow. Translated from Inzhenerno-Fizicheskii Zhurnal, Vol. 58, No. 4, pp. 573-577, April, 1990. Original article submitted November 1, 1988.